Electronic Supplementary Material (ESI) for Physical Chemistry Chemical Physics.

Supporting Information for: A Report of Emergent Uranyl Binding Phenomena by an Amidoxime Phosphonic Acid Co-Polymer

C. W. Abney,[a]* S. Das,[a] R. T. Mayes,[b] L.-J. Kuo,[b] J. Wood,[b] G. Gill,[b] M. Piechowicz,[c] Z. Lin,[c] W. Lin,[c] and S. Dai,[a]

[a.] Oak Ridge National Laboratory, P.O. Box 2008, Oak Ridge, Tennessee 37831-6181, United States
[b.] Marine Sciences Laboratory, Pacific Northwest National Laboratory, Sequim, Washington, 98382, United States
[c.] The University of Chicago, 929 East 57th Street, Chicago, Illinois 60637, United States

abneycw@ornl.gov

Section Page

1. Experimental

1.1 General Experimental

All chemicals were obtained from Fisher Scientific or Sigma Aldrich. Uranyl acetate dihydrate was obtained from Ted Pella, Inc. and used without purification as a standard, as well as to prepare uranyl nitrate according to a literature procedure.[1] All other chemicals and solvents were used without further purification or treatment. AI-8 adsorbent fibres prepared by RIGP were prepared as previously reported in the literature, but are labeled as AI-11 in the aforementioned publication.[2] Adsorbent was contacted for 42 days with filtered seawater from the Sequim Bay at PNNL, following activation with KOH for 1 hr.[3, 4] Details pertaining to the KOH activation procedure are provided in section 1.3.1.

Elemental concentration data were obtained with either a PerkinElmer Optima 2100DV ICP-OES (brine solutions), or a Perken Elmer 7300DV ICP-AES (digested polymers), as reported previously.[5] For AI-8 contacted with uranium brine solutions, fibres were collected by filtration, washed with DI water, and dried for 24 hrs under vacuum. A uranium uptake of 185 g U / kg adsorbent was determined by ICP-OES by determining the difference in uranium concentration between the stock solution and supernatant after sorption. For seawater-contacted samples, the adsorbents were rinsed with DI water to remove accumulated salts, dried overnight at 80 °C, massed, digested in 5 mL solution of 50% aqua regia for 2.5 hr at 85 °C. This digest solution was analyzed for uranium and trace elements by ICP-AES. Both instruments were calibrated against a 6-point standard curve with solutions ranging from 0 to 10 ppm. The correlation coefficient was > 0.995 for all analyses of interest.

1.2 Synthesis of Small Molecule Standards

A detailed synthesis and characterization of all small molecule standards was previously published in the literature.[6, 7] Slight modifications to these protocols and specific characterization data were previously reported and can be found in the supporting information of a recent publication.[8]

1.3 Preparation of Polymer Fibres

1.3.1 KOH Pre-treatment of AI-8 Adsorbent Treatment of AI-8 adsorbent with KOH solution prior to deployment is known to dramatically improve uranyl sorption.[9-13] Pre-treatment of the pristine AI-8 was

performed by the same protocol used to pre-treat fibres prior to seawater testing at PNNL.[4] 25 mg (dry weight) fibres were soaked in 25 mL of an aqueous 2.5% KOH solution at 80 °C for 1 hr. The fibres were collected by gravity filtration; to preserve the fibre hydrogel, vacuum was not pulled on the fibres at any point. Fibres were washed extensively with DI water until their pH returned to 7-8. Fibres were stored in DI water at pH 7-8 until use.

1.3.2 Sorption of Uranium by KOH-Treated AI-8 in Brine Solution Following KOH treatment, batches of AI-8 were used to extract uranium from brine solution, the composition of which is provided in Table S1.[3, 4] To minimize the necessary contact time, uranium is added at a concentration of 8 ppm rather than the environmental concentration of 3.3 ppb. No competing metal ions were added to the seawater simulant solutions. KOH-treated AI-8 fibres (25 mg dry weight, prior to KOH treatment) were suspended at a phase ratio of 25 mg L^{-1} in the two seawater simulant solutions and agitated at 200 RPM on a plate shaker for 24 hrs contact time.

Table S1 Composition of Uranium Brine[3, 4]

Chemical	**Mass (L^{-1})**
$UO_2(NO_3)_2 \cdot 6\ H_2O$	17 mg
NaCl	25.6 g
$NaHCO_3$	194 mg

1.3.3 Treatment of Environmental Seawater-Contacted AI-8 Samples of AI-8 adsorbent were contacted with filtered environmental seawater from Sequim Bay in flow-through experiments performed at PNNL, as published previously.[4] In short, fibres were pre-treated with KOH as discussed above, rinsed with DI water, and deployed in flumes for exposure to seawater. After 42 days contact time, the samples were rinsed with DI water to remove salts and stored in DI water until sample preparation. Several notable changes were made to the previously published protocol. A 150 μm inline filter, instead of a 45 μm inline filter, was used to remove fine particulate matter from the environmental seawater prior to contact with the AI-8. The flume was also wrapped with black plastic to suppress any influence of biofouling on metal adsorption.[5]

Seawater is known to contain significant quantities of ions capable of competing with uranium for binding sites. Table 2 displays the concentration of metals in the environmental seawater, as well as previously reported amounts adsorbed by polymer fibres of similar formulation.[4] One environmental sample was prepared for XAFS analysis "as received," while a second sample was stripped of weakly-bound transition metals.[14, 15] To perform the elution process, 2 g AI-8 (wet-mass, as received) were washed with DI water and collected by gravity filtration. They were subsequently immersed in 22.5 mL of an aqueous 0.05 M HCl solution and heated overnight at 30 °C. The adsorbent was collected by gravity filtration and washed with DI water. Both batches of AI-8, as received and post-elution, were first dried on a Buchner funnel, then dried under vacuum for 24 hrs. Each batch yielded ca. 65 mg dry fibres. Dry seawater-exposed samples were digested and analyzed by ICP-AES to determine the quantity of uranium, vanadium, and other metals, as discussed in Section 1.1.

Table S2 Concentration of Metals in Field Test Seawater and as Adsorbed by AI-8

Element	**Filtered Seawater (ng/kg)**	**Transition Metals on AI-8 (mg Metal / g Fibre)**		
		Lit.	Seawater (As Received)	
			mg / g	μmol / g
V	1480	5.7	7.0 ± 0.8	137
U	2840	2.7	2.8 ± 0.04	12
Fe	2200	1.9	4.02 ± 0.09	72
Cu	540	1.3	0.47 ± 0.01	7
Ni	560	0.7	0.44 ± 0.01	7
Zn	2100	0.7	0.65 ± 0.01	10
Sr	---	0.3	< 0.1	< 1
Cr	180	0.2	< 0.1	< 2
Mn	1200	0.1	0.88 ± 0.01	16

Uncertainties for seawater-contacted samples were determined from the standard deviation of two separate analyses, with the average value presented in the above table.

2. X-ray Absorption Fine Structure Spectroscopy

2.1 Preparation of XAFS Standards

The mass of uranium needed to achieve a 1 – 2.5 absorption length edge step was calculated for each small molecule standard based on the elemental composition and mass absorption coefficient for each element.[16] Small molecule standards were dried under vacuum for 1 hr, ground with an agate mortar and pestle, and blended with D-(+)-Glucose to the appropriate concentration.

For each XAFS sample, approximately 35 mg dry AI-8 adsorbent was dried overnight in a vacuum oven at 40 °C overnight. The samples were then immersed in liquid nitrogen and ground with a mortar and pestle until fully pulverized. XAFS samples were prepared without any further dilution. Approximately 20 – 25 mg of sample was enclosed within a nylon washer of 4.953 mm inner diameter (area of 0.193 cm^2), sealed on one side with transparent "Scotch" tape. The sample was pressed thoroughly by hand to form a firm, uniform pellet, then sealed on the open side with a second piece tape. The entire sample was placed into a Mylar baggie. Small pieces of Kapton tape were used to seal the three open edges of the Kapton baggie. This method was approved in advance by the APS Radiation Safety Review Board for achieving the double containment necessary for analysis of radioactive samples.

2.2 Data Collection

The X-ray absorption data were collected at Beamline 10BM-B at the Advanced Photon Source (APS) at Argonne National Laboratory. Spectra were collected at the uranium L_3-edge (17166 eV). Data for small molecule crystal standards and brine-exposed AI-8 adsorbent were collected in transmission mode, while data for seawater-exposed AI-8 were collected by a Hitachi Vortex-ME4 four-element silicon drift fluorescence detector. The X-ray white beam was monochromatized by a Si(111) monochromator and detuned by 50% to reduce the contribution of higher-order harmonics to below the level of noise. The K-edge of an yttrium foil (17038 eV) was used as the reference for energy calibration and measured simultaneously for all samples. The incident beam intensity (I_0), transmitted beam intensity (I_t), and

reference (I_r) were all measured by 20 cm ionization chambers with gas compositions of 80% N_2 and 20% Ar, 95% Ar and 5% N_2, and 100% N_2, respectively. All spectra were collected at room temperature.

Samples were centered on the beam and adjusted to find the most homogeneous location in the sample for data collection. The beam was reduced to dimensions of 400 × 3100 μm for all data collection. Data were collected over six regions: -250 to -30 eV (10 eV step size, dwell time of 0.25 seconds), -30 to -5 eV (5 eV step size, dwell time of 0.5 seconds), -5 to 30 eV (1 eV step size), 3 $Å^{-1}$ to 6 $Å^{-1}$ (0.05 $Å^{-1}$ step size, dwell time of 2 seconds), 6 $Å^{-1}$ to 9 $Å^{-1}$ (0.05 $Å^{-1}$ step size, dwell time of 4 seconds), and 9 $Å^{-1}$ to 15 $Å^{-1}$ (0.05 $Å^{-1}$ step size, dwell time of 8 seconds). Three scans were collected at room temperature (~25°C) for each sample.

The data were processed and analyzed using the Athena and Artemis programs of the IFEFFIT package based on FEFF 6.[17, 18] Reference foil data were aligned to the first zero-crossing of the second derivative of the normalized μ(E) data, which was subsequently calibrated to the literature E_0 for the yttrium K-edge (17038 eV). Spectra were averaged in μ(E) prior to normalization. The background was removed and the data were assigned an Rbkg value of 1.0.

3. EXAFS Fitting

All data were initially fit with k-weighting of 1,2, and 3, then finalized with k^3-weighting in R-space. Structural parameters that were determined by the fits include the degeneracy of the scattering path (N_{degen}), the change in half-path length, R_{eff} (ΔR_i), the relative mean square displacement of the scattering element (σ^2_i), the passive electron reduction factor (S_0^2), and the energy shift of the photoelectron, (ΔE_0). S_0^2 was found to converge to 1.0 ± 0.10 for all fits (standards and polymer fibres) and was thus fixed at that value for all models. Two different ΔE values were used, one for the tightly-bound axial oxygen and the second for all other scattering paths.[19, 20] For each fit, the fit range (ΔR), data range (Δk), number of independent points (N_{idp}), number of variables (N_{var}), degress of freedom (ν), reduced chi-squared value (χ_ν^2), and R-factor (R) are in Table S3. For each fit, the number of independent points was not permitted to exceed 2/3 the number of variables, in keeping with the Nyquist criterion.[20, 21]

Table S3 Data range and goodness-of-fit parameters for best-fit models[a.]

Sample	ΔR (Å)	Δk (Å^{-1})	N_{idp}	N_{var}	ν	χ_ν^2	*R* (%)
UO_2(Benzamidoxime)$_2$	1 – 4.0	2.5 – 14.0	21	12	9	84.0	1.2
UO_2(Glutarimidedioxime)$_2$	1 – 4.0	2.3 – 14.0	22	14	8	132	2.0
AI-8 in Brine (no cyclic)	1 – 4.0	2.2 – 15.1	24	16	8	59.4	1.1
AI-8 in Brine (30% cyclic)	1 – 4.5	2.6 – 15.1	24	16	11	70.0	1.3
AI-8 from Seawater (as received)	1 – 3.5	2.0 – 13.8	18	12	6	17.1	1.4

[a.] Fits of the EXAFS data for both small molecule standards were reported previously in reference 8.

3.1 Small Molecule Standards

Fits of the EXAFS spectra for uranyl benzamidoxime and uranyl glutarimidedioxime were reported in detail previously.[8]

3.2 AI-8 Adsorbent

Fits of AI-8 data were attempted in a bottom-up fashion using models representative of each of the four proposed binding configurations. Fitting atomic degeneracy was achieved through the introduction of a variable which scaled the amplitude reduction factor, S_0^2. While more distant scattering paths were progressively included, refined values for previously established scattering paths were used as initial guesses, but allowed to vary freely to avoid introduction of systematic error. For all models, equatorial light scatterers converged to approximately 5-6 atoms, consistent with previous XAFS and crystallographic studies. Scattering paths, obtained from crystal structures reported in the literature, were added one at a time for different elements at different distances and evaluated in the real-space component of the Fourier transform. Paths which required indefensible changes in scatterer half-path length or mean squared relative deviation were discarded. Paths representative of carbonate were investigated for all polymer fibres, while paths representative of phosphates and a μ^2-oxo bridging Fe cation were considered for all seawater-contacted samples. Iterative refinement of the fits resulted in the finalized models discussed below.

3.2.1 Brine-Contacted AI-8, No Cyclic Contribution The model used to fit the fibre data was composed of several shells of light scattering elements. The first shell was composed exclusively of the tightly-bound uranyl axial oxygen (O_{yl}) with degeneracy fixed at 2. The second shell was composed of light scatterers at two different distances with equal, but variable degeneracy (O_1, N_1). The third shell was

composed of light scatterers at different distances with equal, but variable degeneracy (N_2, C_{CO3}, C). ΔR was a free parameter for all direct scattering paths, and each shell of atoms shared a common σ^2 variable. Degeneracy was a free parameter for all direct scattering paths except O_{yl}. This model is consistent with an average uranyl coordination environment consisting of 2 chelating amidoximes, 0.5 aqua ligands, and 0.5 carbonate.

Table S4 Initial Path Lengths, Degeneracies, and Parameters for Fitting AI-8 Contacted with Brine (No Cyclic Contribution)

Scattering Path	**N_{degen}**	**R(Å)**	**ΔR (Å)**	**σ^2 (Å^2)**	**ΔE_1**
$U \rightarrow O_{yl}$	2	1.79	$\Delta R\text{-}O_{yl}$	$\sigma^2\text{-}O_{yl}$	ΔE_1
$U \rightarrow O_1$	CN_1	2.43	$\Delta R\text{-}O$	$\sigma^2\text{-}1$	ΔE_2
$U \rightarrow N_1$	CN_1	2.53	$\Delta R\text{-}N_1$	$\sigma^2\text{-}1$	ΔE_2
$U \rightarrow C_{CO3}$	CN_2	2.92	$\Delta R\text{-}C_{CO3}$	$\sigma^2\text{-}2$	ΔE_2
$U \rightarrow N_2$	CN_3	3.36	$\Delta R\text{-}N_2$	$\sigma^2\text{-}2$	ΔE_2
$U \rightarrow C$	CN_3	3.47	$\Delta R\text{-}C$	$\sigma^2\text{-}2$	ΔE_2
$U \rightarrow O_{yl(1)} \rightarrow O_{yl(2)}$	2	3.57	$2 \times \Delta R\text{-}O_{yl}$	$2 \times \sigma^2\text{-}O_{yl}$	ΔE_1
$U \rightarrow O_{yl(1)} \rightarrow U \rightarrow O_{yl(2)}$	2	3.57	$2 \times \Delta R\text{-}O_{yl}$	$2 \times \sigma^2\text{-}O_{yl}$	ΔE_1
$U \rightarrow O_{yl(1)} \rightarrow U \rightarrow O_{yl(1)}$	2	3.57	$2 \times \Delta R\text{-}O_{yl}$	$2 \times \sigma^2\text{-}O_{yl}$	ΔE_1

3.2.2 Brine-Contacted AI-8, 30% Cyclic Contribution Similar to the model discussed in Section 3.2.1, the fibre data were fit with several shells of light scattering elements. Scattering paths representative of uranyl bound by a cyclic amidoxime functionality were obtained from the crystallographic information file for the [UO_2(glutarimidedioximate)$_2$] crystal structure, reported previously.[7] The scattering from the imide nitrogen was previously determined to be a characteristic spectroscopic feature, unique to this binding mode.[8] Accordingly, the contribution from the imide nitrogen was fixed at 0.6 atoms per uranium, which would afford a 30% total contribution to the EXAFS spectrum.

The first shell was composed exclusively of the tightly-bound uranyl axial oxygen (O_{yl}) with degeneracy fixed at 2. The second shell was composed of light scatterers at two different distances with equal, but variable degeneracy (O_1, O_2), as well as the imide nitrogen (N_{imide}) with degeneracy fixed at 0.6. The third shell was composed of light scatterers at different distances with equal, but variable degeneracy

(N, C_{CO3}, C). ΔR was a free parameter for all direct scattering paths, and each shell of atoms shared a common σ^2 variable. Degeneracy was a free parameter for all direct scattering paths except O_{yl} and N_{imide}.

Table S5 Initial Path Lengths, Degeneracies, and Parameters for Fitting Polymer Fibres Contacted with Seawater Simulant (Fixed 30% Cyclic Contribution)

Scattering Path	**N_{degen}**	**R(Å)**	**ΔR (Å)**	**σ^2 (Å^2)**	**ΔE_1**
$U \rightarrow O_{yl}$	2	1.79	$\Delta R\text{-}O_{yl}$	$\sigma^2\text{-}O_{yl}$	ΔE_1
$U \rightarrow O_1$	CN_1	2.30	ΔR-O	σ^2-1	ΔE_2
$U \rightarrow O_2$	CN_1	2.30	ΔR-O	σ^2-1	ΔE_2
$U \rightarrow N_{imide}$	0.6	2.45	$\Delta R\text{-}N_{imide}$	σ^2-2	ΔE_2
$U \rightarrow C_{CO3}$	CN_2	3.47	$\Delta R\text{-}C_{CO3}$	σ^2-3	ΔE_2
U→N	CN_3	3.31	ΔR-N	σ^2-3	ΔE_2
U→C	CN_3	3.47	ΔR-C	σ^2-3	ΔE_2
$U \rightarrow O_{yl(1)} \rightarrow O_{yl(2)}$	2	3.57	$2 \times \Delta R\text{-}O_{yl}$	$2 \times \sigma^2\text{-}O_{yl}$	ΔE_1
$U \rightarrow O_{yl(1)} \rightarrow U \rightarrow O_{yl(2)}$	2	3.57	$2 \times \Delta R\text{-}O_{yl}$	$2 \times \sigma^2\text{-}O_{yl}$	ΔE_1
$U \rightarrow O_{yl(1)} \rightarrow U \rightarrow O_{yl(1)}$	2	3.57	$2 \times \Delta R\text{-}O_{yl}$	$2 \times \sigma^2\text{-}O_{yl}$	ΔE_1

3.2.3 Seawater-Contacted AI-8 (As Received) The model used to fit the fibre data was composed of several shells of light scattering elements and one transition metal scatterer. The first shell was composed exclusively of the tightly-bound uranyl axial oxygen (O_{yl}) with degeneracy fixed at 2. The second shell was composed of light scatterers at two different distances with equal, but variable degeneracy (O_1, N_1). The third shell was composed of one light scatterer with variable degeneracy (N_2) and a transition metal, Fe. ΔR was a free parameter for all direct scattering paths, and degeneracy was a free parameter for all direct scattering paths except O_{yl}. To comply with the Nyquist criterion, the degeneracy for O_1 and N_1 were defined as equivalent, and only one scattering path was used to model both N and C contributions in the third shell. Values for σ^2 were assigned based on whether the elements were light scatterers (O, N, C) or Fe. Fits with more parameters yielded similar values in R-factor, but much larger χ_v^2, in addition to violating the Nyquist criterion. This model structure is most consistent with an average coordination environment consisting of approximately two chelating ligands per uranyl and one μ^2 bridging Fe, however, the large error for Fe coordination number and σ^2 suggests this model is not able to completely describe the data. It

is likely fractional contributions from phosphate, carbonate, and different metal species, are necessary to improve the fit. Data were not fit beyond 3.5 Å in R-space due to the noise in the data.

Table S6 Initial Path Lengths, Degeneracies, and Parameters for Fitting AI-8 Contacted with Brine (No Cyclic Contribution)

Scattering Path	**N_{degen}**	**R(Å)**	**ΔR (Å)**	**σ^2 (Å^2)**	**ΔE_1**
$U \rightarrow O_{yl}$	2	1.79	$\Delta R\text{-}O_{yl}$	$\sigma^2\text{-}O_{yl}$	ΔE_1
$U \rightarrow O_1$	CN_1	2.43	$\Delta R\text{-}O_1$	$\sigma^2\text{-}1$	ΔE_2
$U \rightarrow N_1$	CN_1	2.53	$\Delta R\text{-}N_1$	$\sigma^2\text{-}1$	ΔE_2
$U \rightarrow N_2$	CN_2	3.36	$\Delta R\text{-}N_2$	$\sigma^2\text{-}1$	ΔE_2
$U \rightarrow Fe$	CN_3	3.53	$\Delta R\text{-}Fe$	$\sigma^2\text{-}2$	ΔE_2
$U \rightarrow O_1 \rightarrow N_2$	CN_2	3.53	$0.5 \times \Delta R\text{-}O_1 + 0.5 \times \Delta R\text{-}N_2$	$\sigma^2\text{-}1$	ΔE_2
$U \rightarrow O_{yl(1)} \rightarrow O_{yl(2)}$	2	3.57	$2 \times \Delta R\text{-}O_{yl}$	$2 \times \sigma^2\text{-}O_{yl}$	ΔE_1
$U \rightarrow O_{yl(1)} \rightarrow U \rightarrow O_{yl(2)}$	2	3.57	$2 \times \Delta R\text{-}O_{yl}$	$2 \times \sigma^2\text{-}O_{yl}$	ΔE_1
$U \rightarrow O_{yl(1)} \rightarrow U \rightarrow O_{yl(1)}$	2	3.57	$2 \times \Delta R\text{-}O_{yl}$	$2 \times \sigma^2\text{-}O_{yl}$	ΔE_1

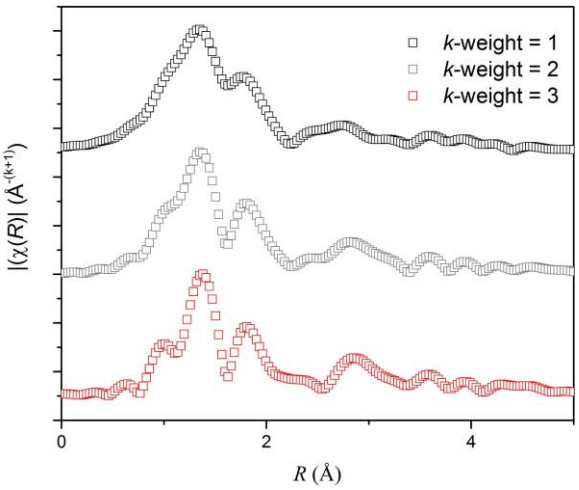

Figure S1. Comparison of seawater-contacted AI-8 with *k*-weighting of 1, 2, and 3. Notably, the feature at 3 Å changes in quadrature as a function of *k*-weighting, consistent with scattering from a heavier element, such as a transition metal.

References:

1. S. P. Kelley, P. S. Barber, P. H. K. Mullins and R. D. Rogers, *Chem. Commun.*, 2014, **50**, 12504-12507.

2. S. Das, Y. Oyola, R. T. Mayes, C. J. Janke, L. J. Kuo, G. Gill, J. R. Wood and S. Dai, *Ind. Eng. Chem. Res.*, 2016, **55**, 4103-4109.

3. J. Kim, Y. Oyola, C. Tsouris, C. R. Hexel, R. T. Mayes, C. J. Janke and S. Dai, *Ind. Eng. Chem. Res.*, 2013, **52**, 9433-9440.

4. J. Kim, C. Tsouris, Y. Oyola, C. J. Janke, R. T. Mayes, S. Dai, G. Gill, L.-J. Kuo, J. Wood, K.-Y. Choe, E. Schneider and H. Lindner, *Ind. Eng. Chem. Res.*, 2014, **53**, 6076-6083.

5. J. Park, G. A. Gill, J. E. Strivens, L.-J. Kuo, R. T. Jeters, A. Avila, J. R. Wood, N. J. Schlafer, C. J. Janke, E. A. Miller, M. Thomas, R. S. Addleman and G. T. Bonheyo, *Ind. Eng. Chem. Res.*, 2016, **55**, 4328-4338.

6. S. Vukovic, L. A. Watson, S. O. Kang, R. Custelcean and B. P. Hay, *Inorg. Chem.*, 2012, **51**, 3855-3859.

7. G. Tian, S. Teat, Z. Zhang and L. Rao, *Dalton. Trans.*, 2012, **41**, 11579-11586.

8. C. W. Abney, R. T. Mayes, M. Piechowicz, Z. Lin, V. Bryantsev, G. M. Veith, S. Dai and W. Lin, *Energy Environ. Sci.*, 2016, **9**, 448-453.

9. S. O. Kang, S. Vukovic, R. Custelcean and B. P. Hay, *Ind. Eng. Chem. Res.*, 2012, **51**, 6619-6624.

10. A. Zhang, T. Asakura and G. Uchiyama, *React. Funct. Polym.*, 2003, **57**, 67-76.

11. S. Katragadda, H. D. Gesser and A. Chow, *Talanta*, 1997, **45**, 257-263.

12. A. Zhang, G. Uchiyama and T. Asakura, *Sep. Sci. Technol.*, 2003, **38**, 1829-1849.

13. N. Seko, A. Katakai, M. Tamada, T. Sugo and F. Yoshii, *Sep. Sci. Technol.*, 2004, **39**, 3753-3767.

14. J. Kim, C. Tsouris, R. T. Mayes, Y. Oyola, T. Saito, C. J. Janke, S. Dai, E. Schneider and D. Sachde, *Sep. Sci. Technol.*, 2013, **48**, 367-387.

15. Y. Kobuke, H. Tanaka and H. Ogoshi, *Polym J*, 1990, **22**, 179-182.

16. B. L. Henke, E. M. Gullikson and J. C. Davis, *At. Data Nucl. Data Tables*, 1993, **54**, 181-342.

17. B. Ravel and M. Newville, *J. Synchrotron Radiat.*, 2005, **12**, 537-541.

18. J. J. Rehr and R. C. Albers, *Rev. Mod. Phys.*, 2000, **72**, 621-654.

19. S. D. Kelly, D. Hesterberg and B. Ravel, in *Methods of Soil Analysis*, eds. A. L. Ulery and L. R. Drees, Soil Science Society of America, Madison, WI, 2008, vol. 5, ch. 14, pp. 387 - 463.

20. S. D. Kelly, K. M. Kemner, J. B. Fein, D. A. Fowle, M. I. Boyanov, B. A. Bunker and N. Yee, *Geochim. Cosmochim. Acta*, 2002, **66**, 3855-3871.

21. S. Calvin, *XAFS for Everyone*, CRC Press, Boca Raton, FL, 2013.